

Research

Unveiling deep Earth's hidden potential: insights from a new high-pressure phase discovered in a shocked meteorite

Luca Bindi¹ · Zhidong Xie² · Thomas G. Sharp³ · Xiande Xie⁴

Received: 11 June 2024 / Accepted: 8 August 2024

Published online: 04 September 2024

© The Author(s) 2024 [OPEN](#)

Abstract

In this study, we report the discovery of a novel high-pressure phase within the Suizhou shocked meteorite, shedding light on the extreme conditions encountered during meteorite impacts. Utilizing advanced analytical techniques including electron microprobe and single-crystal X-ray diffraction, we identified a previously unknown crystalline structure formed under high pressures and temperatures. The new mineral, ideally $\text{Mg}_3(\text{Si}_{0.5}\square_{0.5})\text{Si}_2\text{O}_8$ (the symbol \square stands for structural vacancy), was approved by the International Mineralogical Association (IMA 2024–012) and named ohtaniite in honour of Eiji Ohtani. The phase, a new mineral with the pyroxene chemistry but with wadsleyite structure, was characterized by its distinct crystal lattice and unique physical properties, suggesting a transformation induced by shock compression. This finding expands our understanding of shock-induced mineralogical transformations in extraterrestrial materials and offers insights into the dynamic processes shaping meteorite evolution. Further investigations into these high-pressure phases are crucial for unraveling the geological history of meteorites and their significance in planetary science.

1 Introduction

High-pressure minerals found in shocked meteorites can provide valuable insights into the deep interior of our planet Earth. They provide the natural examples of deep-Earth materials that allow for these important phases to be named and in some cases give clues about the extreme pressure and temperature conditions that may exist deep in planetary mantles. At the same time, laboratory experiments that mimic high-pressure conditions help in understanding the behavior of minerals under extreme environments, and the comparison of experimental data with natural high-pressure minerals help us refine our models of shock processes in meteorite parent bodies. However, there are some limitations in the application of these materials to the Earth. Meteoritic minerals might have compositions or properties that differ from those formed under terrestrial conditions and the direct extrapolation to Earth's deep interior requires careful consideration of these differences. Moreover, the conditions thought to be present in the deep Earth are generally different from those experienced during impact events. The scale, duration, and nature of geological processes in the mantle lead to chemical and textural equilibrium that is not generally produced from the transient shock environments experienced by meteorites. Thus, while high-pressure minerals in shocked meteorites can provide valuable insights into deep Earth

✉ Luca Bindi, luca.bindi@unifi.it; Zhidong Xie, zhidongx@nju.edu.cn; Thomas G. Sharp, tom.sharp@asu.edu; Xiande Xie, xdxie@gzb.ac.cn
| ¹Dipartimento di Scienze Della Terra, Università degli Studi di Firenze, Via G. La Pira 4, 50121 Florence, Italy. ²School of Earth Sciences and Engineering, Nanjing University, 163 Xianlin Road, Qixia District, Nanjing 210023, China. ³School of Earth and Space Exploration, Arizona State University, Tempe, AZ 85287, U.S.A.. ⁴Key Laboratory of Mineralogy and Metallogeny/Guangdong Provincial Key Laboratory of Mineral Physics and Materials, Guangzhou Institute of Geochemistry, Chinese Academy of Sciences, Guangzhou 510640, China.



processes, their application requires careful integration with other data sources, such as experimental petrology, seismology, and geochemistry to contribute to our understanding of Earth's interior and its dynamic evolution.

When studying the Earth's deep mantle, especially in the context of geological processes and material properties, it is crucial to strike a balance between simplification for interpretation and retaining essential complexities. The deep Earth is a highly dynamic and complex system, influenced by various physical and chemical processes that operate over vast spatial and temporal scales. The composition and behavior of materials under extreme pressure and temperature conditions in the mantle are critical. Simplifying material properties too much can lead to inaccurate representations of phenomena like seismic wave propagation, which are key for understanding mantle structure. Deep mantle processes involve complex chemical reactions that influence material properties and phase transitions. Oversimplifying chemical interactions can obscure important aspects of mantle behavior, such as the formation of mineral phases or the recycling of materials through subduction. Interpreting seismic data from the deep mantle requires sophisticated models that account for the heterogeneity of Earth's interior.

Most of the models for our deep Earth are based on well-known upper mantle minerals and their high-pressure polymorphs. We here demonstrate that high-pressure minerals can be much more complex than previously thought. During a mineralogical investigation of the Suizhou meteorite, we discovered a new mineral that appears nearly identical to low-Fe wadsleyite ($M^{2+}:\text{Si} = 2:1$) in back scatter electron images in the scanning electron microscope, but it has a pyroxene stoichiometry ($M^{2+}:\text{Si} = 1:1$) and retains the wadsleyite structure. The mineral was accepted by the International Mineralogical Association (IMA 2024–012) and was named ohtaniite, after Professor Eiji Ohtani. Interestingly, a phase with pyroxene stoichiometry and with olivine structure was discovered in the quenched shock melt from the Tenham L-chondrite [1]. These authors interpreted this phase as a metastable, nonstoichiometric olivine that crystallized from chondritic melt at the edge of a shock vein during rapid quench. The significance of the finding is that olivine can incorporate Si into octahedral coordination at high pressures and temperatures [1]. The occurrence of ohtaniite in Suizhou demonstrates that wadsleyite can also incorporate excess Si in octahedral sites. The similarity to stoichiometric wadsleyite in BSE contrast suggests that ohtaniite may be present in other wadsleyite-bearing shocked chondrites, but previously missed.

1.1 Sample

Ohtaniite was detected as rare subhedral μm -sized grains in a shocked melt pocket of the Suizhou meteorite (Fig. 1). Suizhou L6 chondrite is a shocked meteorite with occurrence of thin shock melt veins less than three hundred micrometers in thickness. The shock veins in Suizhou meteorite contain abundant high-pressure polymorphs including ringwoodite, majorite, majorite-pyropite garnet, akimotoite, magnesiowüstite, lingunite, tuite, xieite, wadsleyite, wangdaodeite, hemleyite, asimowite, elgoresyite and hiroseite [2–15]. A (Mg,Fe)SiO₃-glass was also identified in the shock veins, which was suggested to be possibly a vitrified perovskite [9].

Ohtaniite is associated to Fe-poor (FeO up to 1.50 wt%) and Fe-rich wadsleyite (FeO up to 6.0 wt%), MgSiO₃ glass and Fe–Ni metal. Few grains of wadsleyite (both Fe-poor and Fe-rich fragments) were tested by single-crystal X-ray diffraction and turned out to exhibit the classic features observed in the crystal structure of normal wadsleyite [16]. The ohtaniite fragment used for the X-ray investigation (see below), which was handpicked from the region indicated in the bottom part of Fig. 1, is about $7 \times 9 \times 17 \mu\text{m}$ in size. Colour, lustre, streak, hardness, tenacity, cleavage, fracture, and density could not be determined because of the small grain size. Holotype material of ohtaniite is deposited in the collections of the Museo di Storia Naturale, Università degli Studi di Firenze, Via La Pira 4, I-50121, Firenze, Italy, catalogue number 3238/l.

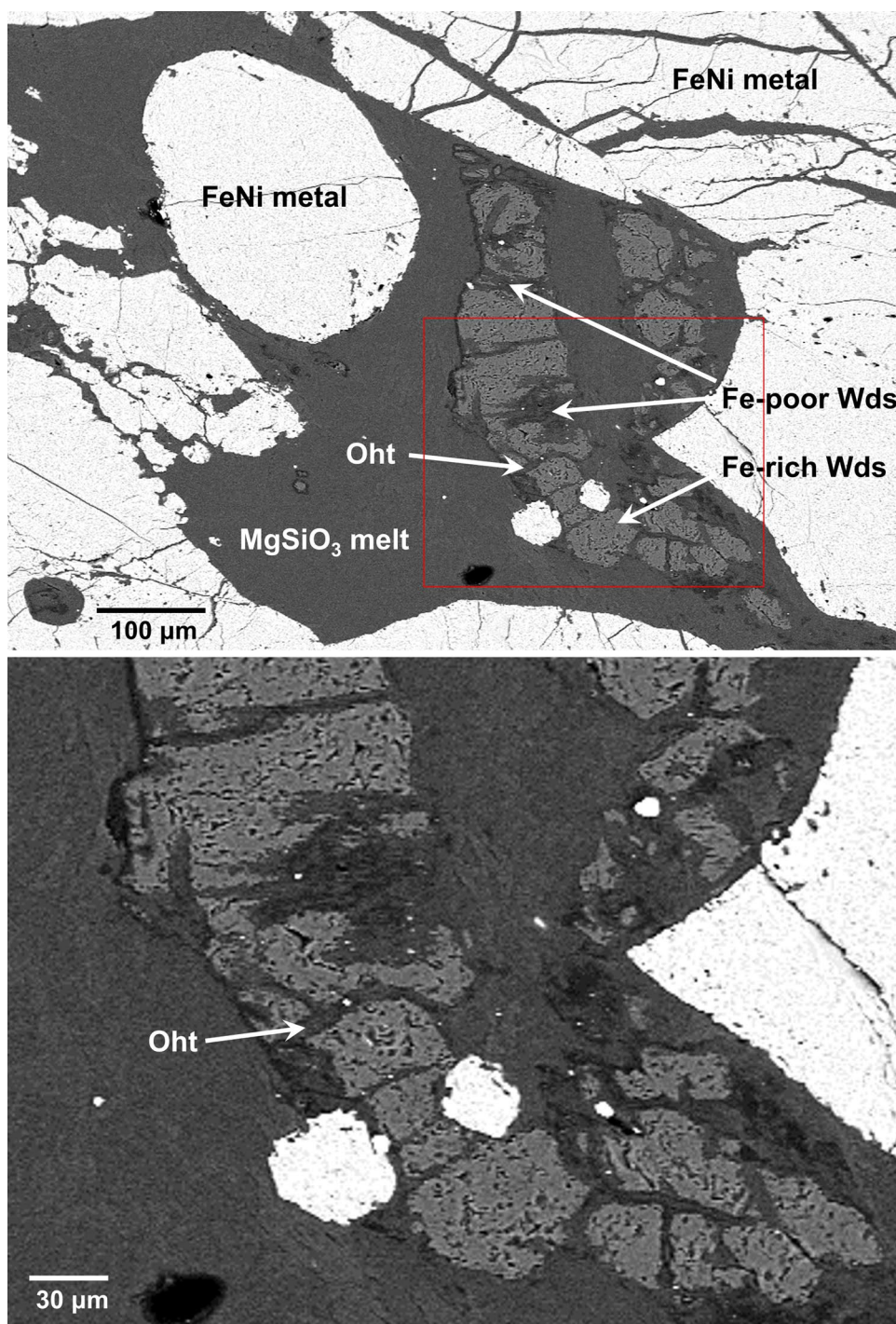
Shock conditions estimated for the Suizhou meteorite are in the P range 18–20 GPa and the shock vein quench represents a T range of 1973–2273 K [11]. On the basis of the coexistence of wadsleyite and ohtaniite (Fig. 1) and according to the P – T diagram of the Allende chondrite [17], we suggest that ohtaniite crystallized from a melt produced by a mixture of partial molten FeNi-metal and silicate at very high temperature > 2000 K and pressure around 18–20 GPa [18].

1.2 Methods

Six separate pieces were cut from a small portion of the Suizhou meteorite, weighing around 10 g. After embedding each piece in epoxy and polishing them using diamond paste, the pieces were examined using electron microprobe and scanning electron microscopy.

A Zeiss-EVO MA15 scanning electron microscope and an Oxford INCA250 energy-dispersive spectrometer were the instruments utilized. They were set up to operate at 25 kV accelerating potential, 500 pA probe current, 2500 cps

Fig. 1 Up: SEM-BSE panoramic image of the section containing ohtaniite. The dashed red rectangular area indicates the region blown up in the BSE image on the bottom panel. Ohtaniite (Oht) is associated with Fe-poor and Fe-rich wadsleyite (Wds), FeNi metal and MgSiO₃ glass. Bottom: blow-up of ohtaniite (Oht) handpicked for the X-ray investigation



as the average count rate across the entire spectrum, and 500 s for counting time. 30-nm-thick carbon film was used for sputter-coating the samples. The preliminary chemical analysis using EDS performed on the crystal fragment used for the structural study did not indicate the presence of elements ($Z > 9$) other than Fe, Mg, Si and minor Na, Al and Ca. Analyses (4 spots) were then carried out using a JEOL 8200 microprobe (WDS mode, 15 kV, 10 nA, 1 μm beam size, counting times 20 s for peak and 10 s for background). For the WDS analyses the $K\alpha$ lines for all the elements were used. The crystal fragment was found to be homogeneous within analytical error.

After the chemical characterization, a small ohtaniite fragment was extracted for the X-ray study from the polished section under a reflected light microscope from the region indicated in the right panel of Fig. 1 and mounted on a

5 μm diameter carbon fiber, which was, in turn, attached to a glass rod. Single-crystal X-ray studies were carried out using a Bruker D8 Venture diffractometer equipped with a Photon III detector using graphite-monochromatized MoK α radiation ($\lambda = 0.71073 \text{ \AA}$). Single-crystal X-ray diffraction intensity data were integrated and corrected for standard Lorentz-polarization factors and absorption with APEX3 [19]. A total of 610 unique reflections were collected. The statistical tests on the distribution of $|E|$ values ($|E^2 - 1| = 1.025$) indicate the presence of an inversion center. Systematic absences agreed with the space group *Imma*. Given the similarity of the unit cell values, space group, and general stoichiometry, the structure was refined using the atomic coordinates given for wadsleyite [16], through Shelxl-2014 [20], up to $R1 = 3.03\%$. Scattering curves for neutral atoms were taken from the *International Tables for Crystallography* [21].

Powder X-ray diffraction data were collected using a Bruker D8 Venture diffractometer equipped with a Photon III detector using CuK α radiation ($\lambda = 1.5418 \text{ \AA}$). The detector-to-sample distance was 7 cm. The program APEX3 [19] was used to convert the observed diffraction rings to a conventional powder diffraction pattern. The least squares refinement gave the following unit-cell values: $a = 5.5902(3)$, $b = 11.416(1)$, $c = 7.7086(5) \text{ \AA}$, $V = 491.93(6) \text{ \AA}^3$.

2 Results and discussion

Electron microprobe analyses of the ohtaniite fragment (Table 1) pointed to the following empirical formula (based on 8 oxygen atoms *pfu*) $[(\text{Mg}_{2.73}\text{Fe}^{2+}_{0.14}\text{Na}_{0.03}\text{Al}_{0.03}\text{Ca}_{0.02}\text{Si}_{0.05})_{\Sigma 3.00}(\text{Si}_{0.49}\square_{0.51})_{\Sigma 1.00}]\text{Si}_2\text{O}_8$, ideally $\text{Mg}_3(\text{Si}_{0.5}\square_{0.5})\text{Si}_2\text{O}_8$ (the symbol \square stands for structural vacancy).

Single-crystal X-ray studies showed the mineral to be orthorhombic, space group *Imma* (#74), with the following unit-cell parameters: $a = 5.5820(10)$, $b = 11.418(3)$, $c = 7.708(2) \text{ \AA}$, $V = 491.3(2) \text{ \AA}^3$ and $Z = 4$. The refinement of the structure, carried out starting from the atom coordinates of wadsleyite [16], converged to $R1 = 3.03\%$ for 412 unique reflections.

In the crystal structure of ohtaniite (Fig. 2), there are four cation sites (three octahedrally coordinated, $M1$, $M2$ and $M3$, and one tetrahedrally coordinated, Si) and four anion sites. Initially, the site occupation factors (s.o.f.) of the four independent cation sites were refined using the following curves: Si vs \square for the $M1$ site; Fe vs Mg for the $M2$ and $M3$ sites, and Si vs \square for the tetrahedrally coordinated site. $M2$ and $M3$ (mean electron numbers of 12.70 and 12.56, respectively) were found to be occupied by Mg with minor Fe; the tetrahedrally coordinated site was found fully occupied by Si and its s.o.f. was fixed to 1. Surprisingly, the $M1$ site was found to exhibit a mean electron number of 7.07, just indicating that about half of the site is vacant (i.e., $[\text{Si}_{0.5}\square_{0.5}]$ site occupancy). The analysis of the polyhedral geometries, together with the comparison with the electron microprobe data, confirmed the site populations inferred by the refined electron densities.

Ohtaniite exhibits the wadsleyite structure. The structure is based on close-packing of cation polyhedra and has extensive edge-sharing octahedra. There is not much room for cation-oxygen-cation angle bending within this structure. However, there are some important differences with respect to wadsleyite mainly related to the fact that Si is present in the usual tetrahedrally coordinated site and the octahedrally coordinated $M1$ site. In detail, Si and structural vacancy are ordered at the octahedrally coordinated site at the origin of the unit cell (Wyckoff position 4a). Ohtaniite can be considered a hyper-silicic wadsleyite but its formula must be written to show that Si is also present at the octahedrally coordinated sites. Crystal-chemical analysis resulted in the possible empirical crystal-chemical formula: $^{M1}(\text{Si}_{0.51}\square_{0.49})_{\Sigma 1.00}^{M2}(\text{Mg}_{0.91}\text{Fe}^{2+}_{0.04}\text{Na}_{0.03}\text{Ca}_{0.02})_{\Sigma 1.00}^{M3}(\text{Mg}_{1.82}\text{Fe}^{2+}_{0.10}\text{Al}_{0.03}\text{Si}_{0.05})_{\Sigma 2.00} \text{Si}_2\text{O}_8$.

The mean $M1$ bond distance, 1.813 \AA , is dramatically shorter than that observed in pure wadsleyite (2.069 \AA ; [16]), while the $M2$ (2.121 \AA) and $M3$ (2.053 \AA) mean bond distances are similar to those in wadsleyite (2.084 and 2.090 \AA ;

Table 1 Compositional data (means and ranges in wt% of oxides), standard deviations (SD) and probe standards used for ohtaniite

Constituent	Mean	Range	SD	Probe Standard
SiO ₂	55.06	54.26–56.14	0.70	Forsterite
Al ₂ O ₃	0.54	0.38–0.91	0.09	Albite
FeO	3.60	3.39–3.98	0.19	Fayalite
MgO	39.39	38.88–40.29	0.35	Forsterite
CaO	0.41	0.30–0.61	0.06	Plagioclase
Na ₂ O	0.34	0.22–0.46	0.10	Albite
Total	99.34	99.09–99.94		

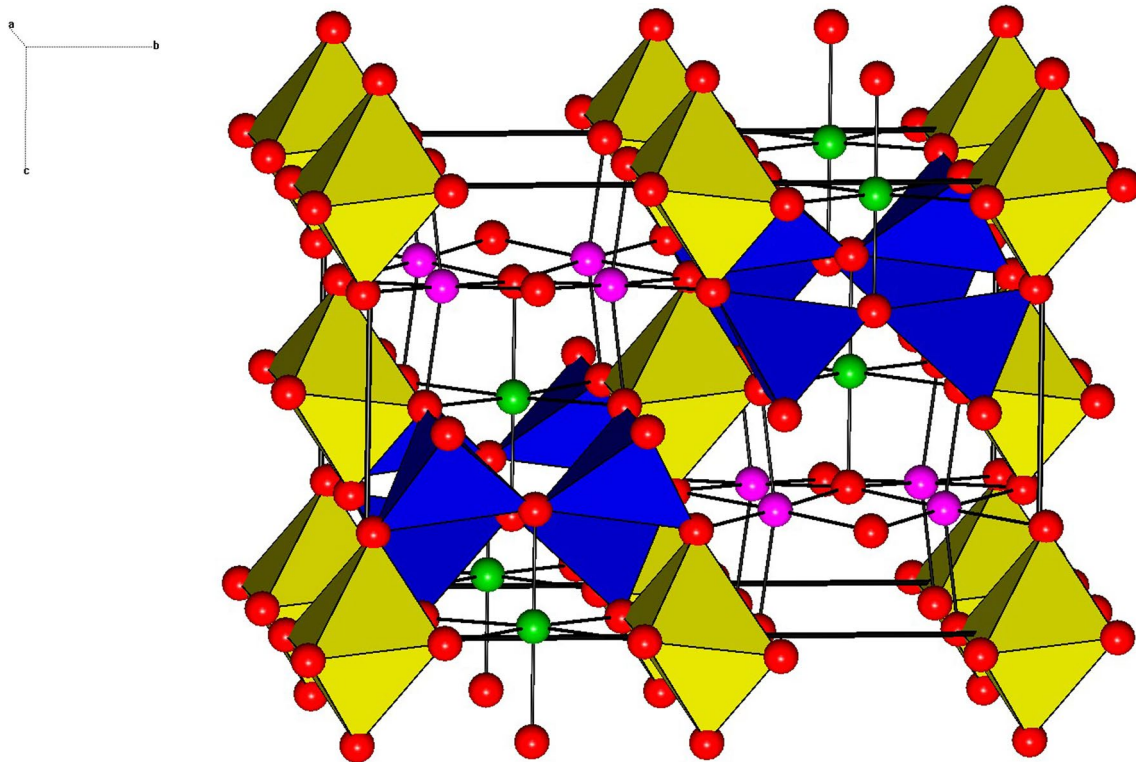


Fig. 2 The crystal structure of ohtaniite down [100] (perspective view). $M1O_6$ polyhedra are depicted as yellow octahedra, whereas $M2$ and $M3$ are indicated with green and violet spheres, respectively. SiO_4 are drawn as blue tetrahedra

[16]). Also, the observed mean tetrahedral distance (1.650 Å) is nearly identical to that observed for wadsleyite (1.651 Å; [16]).

The most striking change in unit-cell values concerns the c -axis, which changes from 8.2566 Å in wadsleyite [16] to 7.708 Å in ohtaniite. Consequently, the unit-cell volume decreases in ohtaniite of about 9% with respect to pure wadsleyite. This feature reflects on the density of ohtaniite which shows a value of 3.728 g/cm³, much denser than pure wadsleyite (3.47 g/cm³; [16]). Interestingly, ohtaniite exhibits a density nearly identical to that of ringwoodite (3.71 g/cm³).

Ohtaniite is a new Mg–silicate with a composition close to that of a pyroxene (formula: $(Mg_{0.99}Fe^{2+}_{0.05}Ca_{0.01}Na_{0.01})_{\Sigma 1.06}(Si_{0.93}Al_{0.01})_{\Sigma 0.94}O_{3.00}$, on the basis of 2 cations) but with the structure of wadsleyite, a polymorph of Mg_2SiO_4 [16]. The mineral somewhat resembles the nonstoichiometric olivine discovered in shock-induced melt veins of the Tenham L6 chondrite by transmission electron microscopy [1]. The chemistry of that phase in Tenham could be written as $Na_{0.06}Ca_{0.02}Mg_{0.71}Fe_{0.20}Al_{0.11}Si_{0.94}O_3$, so close to the $MgSiO_3$ stoichiometry, but diffraction data indicated an olivine structure ($a = 4.78$, $b = 10.11$, and $c = 5.94$ Å). Thus, according to the TEM data, Xie et al. [1] wrote the chemical formula as $(Na_{0.08}Ca_{0.03}Mg_{0.95}Fe_{0.26}Al_{0.15}Si_{0.25}[]_{0.28})_2SiO_4$, with 0.28 formula units of structural vacancies ($[]$), 0.11 of Na plus Ca, and 0.25 of Si, in octahedral sites.

Ohtaniite could be relatively common in shocked chondrites that contain wadsleyite. Indeed, by means of routinely identification methods (e.g. EBSD), it could be misidentified as wadsleyite and, if one uses only the chemical composition it can be misidentified as one of the $MgSiO_3$ polymorphs (enstatite, akimotoite, majorite or bridgmanite). As Raman spectroscopy is the most used method of identifying high-pressure polymorphs in shocked meteorites, it will be important to obtain Raman spectra for ohtaniite for future studies when more samples will be available. Ohtaniite and the super-silicic olivine described in the Tenham L6 chondrite ([1], pyroxene chemistry but olivine structure) underline the possibility of super-silicic olivine polymorphs with excess silicon in octahedral sites. These super-silicic phases formed in shock veins that rapidly quenched from very high temperature. Although this environment is different from the conditions of Earth's mantle, they illustrate an important defect in high-pressure silicates where excess silicon can enter octahedral cation sites.

Acknowledgements SEM studies were conducted at the MEMA laboratory of the University of Florence, Italy. EPMA analyses were carried out at the LaMA laboratory of the University of Florence, Italy. Single-crystal and powder X-ray diffraction studies were done at CRIST, Centro di Cristallografia Strutturale, University of Florence, Italy.

Author contributions LB conceived the project and supervised the study, acquired funding, interpreted the data, wrote the first version of the manuscript. All authors (ZX, TGS, and XX) contributed to the writing of the final version of the manuscript.

Funding This work was supported by “Progetto di Ateneo 2024” of the University of Florence, Italy (L.B.), the National Natural Science Foundation of China under Grant No. 41172046, the Science and Technology Planning Project of Guangdong Province, 2023B1212060048 (X.X.), and the National Natural Science Foundation of China under Grant No. 41272057.

Data availability Crystallographic data (CCDC 2353664) can be obtained free of charge from *The Cambridge Crystallographic Data Centre* via www.ccdc.cam.ac.uk/data_request/cif. Chemical data are reported in the manuscript.

Declarations

Competing interests The authors declare no competing interests.

Open Access This article is licensed under a Creative Commons Attribution-NonCommercial-NoDerivatives 4.0 International License, which permits any non-commercial use, sharing, distribution and reproduction in any medium or format, as long as you give appropriate credit to the original author(s) and the source, provide a link to the Creative Commons licence, and indicate if you modified the licensed material. You do not have permission under this licence to share adapted material derived from this article or parts of it. The images or other third party material in this article are included in the article's Creative Commons licence, unless indicated otherwise in a credit line to the material. If material is not included in the article's Creative Commons licence and your intended use is not permitted by statutory regulation or exceeds the permitted use, you will need to obtain permission directly from the copyright holder. To view a copy of this licence, visit <http://creativecommons.org/licenses/by-nc-nd/4.0/>.

References

1. Xie Z, Sharp TG, Leinenweber K, et al. A new mineral with an olivine structure and pyroxene composition in the shock-induced melt veins of Tenham L6 chondrite. *Am Mineral*. 2011;96:430–6.
2. Xie XD, Chen M, Wang DQ. Shock-related mineralogical features and *P-T* history of the Suizhou L6 chondrite. *Eur J Mineral*. 2001;13:1177–90.
3. Xie XD, Minitti ME, Chen M, et al. Tuite, $\gamma\text{-Ca}_3(\text{PO}_4)_2$, a new phosphate mineral from the Suizhou L6 chondrite. *Eur J Mineral*. 2003;15:1001–5.
4. Xie XD, Chen M, Wang, DQ. Two types of silicate melts in naturally shocked meteorites. In: *Papers and abstracts of the 5th Annual Meeting of IPACES, Guangzhou, 2005*, 12–14.
5. Xie XD, Sun ZY, Chen M. The distinct morphological and petrological features of shock melt veins in the Suizhou L6 chondrite. *Met Plan Sci*. 2011;46:459–69.
6. Xie XD, Gu XP, Yang HX, et al. Wangdaodeite, the LiNbO_3 -structured high-pressure polymorph of ilmenite, a new mineral from the Suizhou L6 chondrite. *Met Plan Sci*. 2020;55:184–92.
7. Chen M, Shu JF, Xie XD, et al. Natural CaTi_2O_4 -structured FeCr_2O_4 polymorph in the Suizhou meteorite and its significance in mantle mineralogy. *Geoch Cosmoch Acta*. 2003;67:3937–42.
8. Chen M, Shu JF, Mao HK, et al. Natural occurrence and synthesis of two new postspinel polymorphs of chromite. *Proc Nat Acad Sci USA*. 2003;100:14651–4.
9. Chen M, Xie XD, El Goresy A. A shock-produced $(\text{Mg, Fe})\text{Si}_3\text{O}_3$ glass in the Suizhou meteorite. *Met Plan Sci*. 2004;39:1797–808.
10. Chen M, Shu JF, Mao H-K. Xieite, a new mineral of high-pressure FeCr_2O_4 polymorph. *Chinese Sci Bull*. 2008;53:3341–5.
11. Chen M, Xie XD. Shock-produced akimotoite in the Suizhou L6 chondrite. *Sci China Earth Sci*. 2015;58:876–80.
12. Bindi L, Chen M, Xie X. Discovery of the Fe-analogue of akimotoite from the shocked Suizhou L6 chondrite. *Sci Rep*. 2017;7:42674.
13. Bindi L, Brenker FE, Nestola F, et al. Discovery of asimowite, the Fe-analogue of wadsleyite, in shock-melted silicate droplets of the Suizhou L6 and the Quebrada Chimborazo 001 CB3.0 chondrites. *Am Mineral*. 2019;104:775–8.
14. Bindi L, Sinmyo R, Bykova E, et al. Discovery of elgoresyite, $(\text{Mg, Fe})_5\text{Si}_2\text{O}_9$: implications for novel iron-magnesium silicates in rocky planetary interiors. *ACS Earth and Space Chem*. 2021;5(8):2124–30.
15. Bindi L, Shim S-H, Sharp TG, et al. Evidence for the charge disproportionation of iron in extraterrestrial bridgmanite. *Sci Adv*. 2020;6:eay7893.
16. Horiuchi H, Sawamoto H. $\beta\text{-Mg}_2\text{SiO}_4$: single-crystal X-ray diffraction study. *Am Mineral*. 1981;66:568–75.
17. Agee CB, Li J, Shannon MC, et al. Pressure-temperature phase diagram for the Allende meteorite. *J Geophys Res*. 1995;100:17725–40.
18. Chen M, Sharp TG, El Goresy A, et al. The majorite-pyroxene + magnesiowüstite assemblage: constraints on the history of shock veins in chondrites. *Science*. 1996;271:1570–3.
19. Bruker. APEX3, SAINT and SADABS. Bruker AXS Inc., Madison, Wisconsin, USA. 2016.
20. Sheldrick GM. Crystal structure refinement with SHELXL. *Acta Crystallogr C*. 2015;71:3–8.
21. Wilson AJC Ed. *International Tables for Crystallography, Volume C: Mathematical, physical and chemical tables*. Kluwer Academic, Dordrecht, NL. 1992.

Publisher's Note Springer Nature remains neutral with regard to jurisdictional claims in published maps and institutional affiliations.